J. Fluid Mech. (2002), *vol.* 454, *pp.* 235–261.
DOI: 10.1017/S0022112001007133 Printed in the United Kingdom

A lubrication model of coating flows over a curved substrate in space

By R. VALÉRY ROY[1], A. J. ROBERTS[2] AND M. E. SIMPSON[2]

[1]Department of Mechanical Engineering, University of Delaware, USA
e-mail: roy@me.udel.edu

[2]Department of Mathematics and Computing, University of Southern Queensland, Toowoomba, Queensland 4352, Australia
e-mail: aroberts@usq.edu.au and simpsonm@usq.edu.au

(Received 20 September 1996 and in revised form 17 September 2001)

Consider the three-dimensional flow of a viscous Newtonian fluid upon an arbitrarily curved substrate when the fluid film is thin as occurs in many draining, coating and biological flows. We drive the lubrication model of the dynamics of the film expressed in terms of the film thickness. The comprehensive model accurately includes the effects of the curvature of the substrate, via a physical multiple-scale approach, and gravity and inertia, via more rigorous centre manifold techniques. This new approach theoretically supports the use of the model over a wide range of parameters and provides a sound basis for further development of lubrication models. Numerical simulations exhibit some generic features of the dynamics of such thin fluid films on substrates with complex curvature: we here simulate a film thinning at a corner, the flow around a torus, and draining of a film down a cylinder. The last is more accurate than other lubrication models. The model derived here describes well thin-film dynamics over a wide range of parameter regimes.

1. Introduction

The importance of thin-film fluid flows in countless industrial and natural processes has led to the development of a variety of mathematical models and numerical simulations. This has increased the understanding of the various complex processes at play, such as the effects of generalized Newtonian and shear-thinning rheology of the liquid (Weidner & Schwartz 1994), of geometric complexity of the substrate (Schwartz & Weidner 1995), of multicomponent mixtures and drying processes (Cairncross, Francis & Scriven 1996), of surface contamination (Schwartz *et al.* 1995, 1996) and roughness (Sweeney *et al.* 1993), of advecting and diffusing contaminants, and of moving substrates. See also, for example, Ruschak (1985), Tuck & Schwartz (1990), Moriarty, Schwartz & Tuck (1991), Moriarty & Schwartz (1992, 1993), Chang (1994), Weidner, Schwartz & Eley (1996) and the extensive review of thin-film flows by Oron, Davis & Bankoff (1997). Examples of industrial applications include the coating processes of autobodies, beverage containers, sheet goods and films, decorative coating and gravure roll coating. Physical applications are also found in the biomedical field such as the liquid films covering the cornea of the eye or protecting the linings of the lungs (Grotberg 1994).

Herein, we consider the slow motion of a thin liquid layer over an arbitrarily curved solid substrate. The fluid is assumed to be incompressible and Newtonian,

constituted of a single component and not significantly contaminated by surfactant. The substrate is stationary. The effects of substrate curvature on the flow of thin liquid layers driven by surface tension were first modelled by Schwartz & Weidner (1995) for two-dimensional geometries. Short-wavelength irregularities of the free surface of the fluid are quickly levelled by surface tension forces, but the long-term evolution of the flow is determined primarily by the curvature of the substrate. Their calculations confirm qualitative observations of the thinning of coating layers at outside corners and of the thickening at inside corners. Schwartz *et al.* (1995) studied the joint effect of substrate curvature and the presence of surfactant and showed that corner defects may be altered significantly by the presence of Marangoni forces. The other pertinent case that has received attention is that of flow on the curved substrate of a cylinder. This is the only case of flow on a curved substrate discussed by Oron *et al.* (1997). We develop here the model for the flow of a thin film of fluid on a generally curved substrate.

The model derived herein exploits the thinness of the fluid layer and leads to a 'lubrication' model of the dynamics whereby the unknown fluid fields are parameterized only by the thickness of the fluid layer. Thus, a considerable simplification of the governing equations is achieved when compared to the full Navier–Stokes equations. Such thin-geometry or long-wave models have previously been derived in many physical contexts, such as in the mechanics of beams, plates and shells (Timoshenko & Woinowsky-Krieger 1959; Roberts 1993), coating flows (Levich 1962; Benney 1966; Roskes 1969; Atherton & Homsy 1976; Tuck & Schwartz 1990), shallow-water waves (Mei 1989), viscous fluid sheets (van de Fliert, Howell & Ockenden 1995), etc. On a flat substrate, the usual model for the evolution of a viscous fluid film's thickness η, driven only by surface tension, is given by the following non-dimensional equation

$$\frac{\partial \eta}{\partial t} \approx -\tfrac{1}{3}\nabla\cdot[\eta^3\nabla\tilde{\kappa}],$$

where $\tilde{\kappa}\approx\nabla^2\eta$ is the curvature of the free surface of the fluid film. Based upon the conservation of fluid and the Navier–Stokes equations, outlined in § 2.1, we derive in § 3 the following model for the evolution of a film on a curved substrate:

$$\frac{\partial \zeta}{\partial t} \approx -\tfrac{1}{3}\nabla\cdot[\eta^2\zeta\nabla\tilde{\kappa} - \tfrac{1}{2}\eta^4(\kappa\boldsymbol{I}-\boldsymbol{K})\cdot\nabla\kappa], \tag{1}$$

where $\zeta=\eta-\frac{1}{2}\kappa\eta^2+\frac{1}{3}k_1k_2\eta^3$ is proportional to the amount of fluid locally above the substrate; $\boldsymbol{K}$ is the curvature tensor of the substrate; k_1, k_2 and $\kappa=k_1+k_2$ are the principal curvatures and the mean curvature of the substrate, respectively; and the ∇-operator is expressed in a coordinate system of the substrate, as introduced in § 2. This model systematically accounts for the curvature of the substrate and that of the surface of the film. It extends the model derived by Schwartz & Weidner (1995) (i) to flows where the substrate curvature has a larger effect on the fluid dynamics; (ii) to a two-dimensional substrate; and (iii) later in equation (51) by systematically incorporating more physical effects into the modelling. Our model applies to a wide range of thin fluid film flows in the lubrication approximation.

The flow of a thin fluid on the surface of a cylinder is a situation of long-standing interest. Applications of the model (51) may be to the liquid lining of cylindrical tubes investigated by Jensen (1997) and the formation of drops during coating as explored by Kalliadasis & Chang (1994) and Kliakhandler, Davis & Bankoff (2001). They find that a thin film may form into drops on the fibre, or may saturate into solitary waves depending upon the film thickness. The version of (51) specific of axisymmetric flow

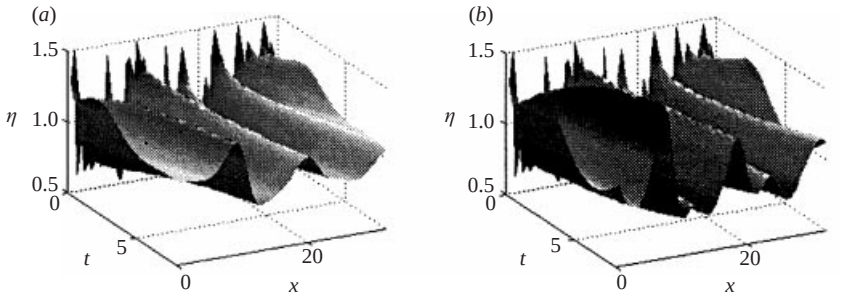

FIGURE 1. Side by side comparison of the evolution of a flow predicted by (*a*) our model (2) and (*b*) Frenkel's model for the axisymmetric draining flow down a cylinder (for non-dimensional parameters $a = Bo = 1$), periodic in x and starting from a random fluid thickness. See the significant differences in the predicted phase speeds and amplitudes of the roll waves $\eta(x,t)$.

around a circular cylinder of radius a is

$$\frac{\partial\zeta}{\partial t} + \frac{1}{3}\frac{\partial}{\partial x}\left[Bo\eta^3\left(1+\frac{\eta}{a}\right) + \eta^2\zeta\left(\frac{1}{a^2(1+\eta/a)^2}\frac{\partial\eta}{\partial x} + \frac{\partial^3\eta}{\partial x^3}\right)\right] \approx 0, \tag{2}$$

in our non-dimensionalization, where x measures axial distance, Bo is a Bond number characterizing axial gravity, and here $\zeta = \eta + \eta^2/2a$. This is approximately the model used by Kalliadasis & Chang (1994) as derived by Frenkel (1992) (replace $1+\eta/a$ by 1 and ζ by η to obtain Frenkel's model). The differences are that their model (Kalliadasis & Chang equation (2)) does not conserve fluid, while our systematic model, equation (2), does and additionally accounts for more physical effects and interactions. Significant qualitative effects are seen in figure 1: the greater influence of surface tension in (2) leads to reduced height but greater speed of the roll waves; and the $1/(1+\eta/a)^2$ factor in (2) is crucial in more accurately predicting a longer wavelength. See § 5.3 for details of these comparisons and the non-axisymmetric model on a cylinder.

The general model, equation (51), reported in § 4.2, also subsumes that of Wilson & Duffy (1998) for the steady draining of a rivulet by generalizing the model to the unsteady flow on general substrate variations.

In order to make such comparisons, we derive the necessary modifications to the model (equation (1)) in § 4 by including gravity and inertia processes in the analysis. Computer algebra, based on centre manifold theory (Roberts 1988), assures us that all relevant dynamical effects and their interactions are incorporated into the model. In centre manifold theory, competing small effects need not appear at leading order in the analysis; thus, we obtain the flexibility to adapt the model to a variety of parameter regimes without redoing the entire analysis (Roberts 1997, for example). The need to do this has been identified not only by Frenkel & Indireshkumar (1997) in their derivation of a generally valid model for thin fluid films flowing down an inclined plane, but also in the review by Oron *et al.* (1997 p. 958) of models for free thin fluid films. Here, the various regimes of gravitational forcing around a curved surface are all encompassed within the one model, namely equation (51). Terms affected by fluid inertia appear very small in generic situations, see (52), and perhaps are best used to indicate the error in the lubrication models for moderate Reynolds number flows – Oron *et al.* (1997 p. 975) indicated that such high-order terms would be useful indicators of errors in an asymptotic model. The centre manifold approach supports the model in equation (1) whether the substrate has constant mean curvature, such as

spheres or cylinders (§ 5.3), when the leading-order dynamics are driven by variations in the thickness of the film, or whether the substrate has varying mean curvature, such as on a torus (§ 5.4) or around a corner (§ 5.2), when the leading-order dynamics are driven by the substrate curvature, see § 5.1. In the latter cases, the leading-order model is structurally unstable and thus it is essential to incorporate higher-order terms into the model. That notionally higher-order terms balance notionally lower-order terms is not necessarily 'a failure ... to represent a rightful limiting case' (Oron *et al.* 1974) but the natural expression that different physical interactions are dominant. The centre manifold approach assures us that models are developed which account, up to some order, for all physical interactions expressed in the original mathematical description of the physical problem.† Centre manifold theory provides a more powerful basis for modelling dynamics. Incorrect initial conditions for dynamical models have often been assumed without comment. Instead, remarkably, in shear dispersion in a channel, the initial condition for the Taylor model of the cross-channel average concentration is not the cross-channel average of the initial concentration (Watt & Roberts 1995); and the initial condition for a finite-difference numerical model is not the grid values of the initial field (Roberts 2001). The geometry of centre manifold theory provides a rational derivation of initial conditions for a model (Cox & Roberts 1995; Roberts 2000). For the flow of a thin film of fluid on a flat substrate, a first analysis (Suslov & Roberts 1998) derives that the initial profile for the lubrication model is not the initial fluid thickness but

$$\eta_0 \approx h_0 - \nabla \cdot \overline{\boldsymbol{u}_0 y(h_0 - \tfrac{1}{2}y)}, \tag{3}$$

where the overbar denotes a cross-film average, $h_0(x)$ is the initial thickness and $\boldsymbol{u}_0$ the initial lateral velocity field of the fluid. Suslov & Roberts (1998) discuss six examples and how the projection, equation (3), matches physical intuition. Generalizing (3) to a curved substrate is for further research. Centre manifold theory further provides a rational derivation of the effects of forcing upon a dynamical model (Cox & Roberts 1995) and of boundary conditions to be applied at the lateral boundaries of a thin domain model (Roberts 1992) such as lubrication theory. Traditional modelling approaches, such as the method of multiple scales, do not provide such a rational treatment of initial and boundary conditions. Thus, using centre manifold theory here is a necessary step in developing fluid dynamics modelling.

In § 5, we describe some numerical simulations of flows on curved surfaces. Attention is given to the quantitative differences found between our model and that obtained by Schwartz & Weidner (1995), and the axisymmetric model on a cylinder by Kliakhandler *et al.* (2001).

2. The fluid equations in the substrate coordinate system

The fluid equations are best analysed and solved in a coordinate system that naturally fits the curving substrate. Based upon the principal directions of curvature of the substrate, we construct an orthogonal curvilinear coordinate system in the neighbourhood of the substrate $\mathscr{S}$. The Navier–Stokes equations, introduced next,

† For a simple example, centre manifold theory guarantees $\dot{x} = \epsilon x - x^3 + O(\epsilon^4 + x^4)$ is a good model of the dynamical system $\dot{x} = \epsilon x - xy$, $\dot{y} = -y + x^2$ irrespective of whether $x = O(\sqrt{\epsilon})$, as it is near the stable fixed point, or whether x is significantly larger, when the equation's balance is dominantly between $\dot{x}$ and $-x^3$ or indeed smaller, when the balance is dominated by $\dot{x}$ and ϵx. Analogously, Ribe (2001) uses a 'composite' model to describe uniformly different asymptotic regimes of the dynamics of a thin viscous sheet.

are analysed in this special coordinate system. This natural coordinate system has some remarkable properties which make a systematic analysis tractable.

2.1. *Equations of motion and boundary conditions*

We solve the Navier–Stokes equations for an incompressible Newtonian fluid of density ρ and viscosity μ moving with velocity field $\boldsymbol{u}$ and pressure field p. The flow is primarily driven by pressure gradients along the substrate and caused by capillary forces characterized by surface tension σ and varying due to variations of the curvature of the free surface of the fluid. In § 4, we include in the analysis a gravitational body force, $\boldsymbol{g}$, of magnitude g in the direction of the unit vector $\hat{\boldsymbol{g}}$.

Suppose the film has characteristic thickness H. We non-dimensionalize the equations by scaling variables with respect to the reference length H, the reference time $\mu H/\sigma$, the reference velocity $U = \sigma/\mu$, and the reference pressure σ/H. Thus, in this non-dimensionalization, we take the view of a microscopic creature of a size comparable to the thickness of the fluid; later, we require that both the substrate and the free surface curve only gently when viewed on this microscale. The non-dimensional fluid equations are then

$$\nabla \cdot \boldsymbol{u} = 0, \tag{4}$$

$$Re\left[\frac{\partial \boldsymbol{u}}{\partial t} + \boldsymbol{u} \cdot \nabla \boldsymbol{u}\right] = -\nabla p + \nabla^2 \boldsymbol{u} + Bo\hat{\boldsymbol{g}}, \tag{5}$$

where $Re = \sigma\rho H/\mu^2$ is effectively a Reynolds number characterizing the importance of the inertial terms – it may be written as UH/ν for the above reference velocity – and $Bo = \rho g H^2/\sigma$ is a Bond number characterizing the importance of the gravitational body force when compared with surface tension.

In § 3, we assume that the regime of the flow is characterized by a very small value of the Reynolds number so that the inertia term $Re\mathrm{D}\boldsymbol{u}/\mathrm{D}t$ is neglected in comparison to the viscous forces in the fluid: $Re = UH/\nu \ll 1$. This is the 'creeping flow' assumption of lubrication. Later, in § 4, we reinstate inertia into the analysis and determine its leading-order effects on the dynamics.

The boundary conditions are as follows.

(i) The fluid immediately in contact with the substrate does not slip along the stationary substrate $\mathscr{S}$, that is

$$\boldsymbol{u} = \boldsymbol{0} \quad \text{on} \quad \mathscr{S}. \tag{6}$$

(ii) The kinematic boundary condition at the free surface of the fluid states that fluid particles must follow the free surface.

(iii) The free surface, denoted by $\mathscr{F}$ and assumed free of contamination, must have zero-shear (tangential stress), namely

$$\tilde{\boldsymbol{\tau}} \cdot \tilde{\boldsymbol{t}}_1 = \tilde{\boldsymbol{\tau}} \cdot \tilde{\boldsymbol{t}}_2 = 0 \quad \text{on} \quad \mathscr{F}, \tag{7}$$

where $\tilde{\boldsymbol{\tau}}$ is the deviatoric stress acting across $\mathscr{F}$, and $\tilde{\boldsymbol{t}}_\alpha$ are independent tangent vectors to $\mathscr{F}$. This condition assumes a light and inviscid medium (such as air) external to the fluid layer.

(iv) Surface tension creates a jump in the normal stress across $\mathscr{F}$ proportional to the mean curvature of $\mathscr{F}$: in non-dimensional form

$$p = -\tilde{\kappa} + \tilde{\boldsymbol{\tau}} \cdot \tilde{\boldsymbol{n}} \quad \text{on} \quad \mathscr{F}, \tag{8}$$

where p is the fluid pressure relative to the assumed zero pressure of the external medium, and $\tilde{\boldsymbol{n}}$ is the unit normal to $\mathscr{F}$.

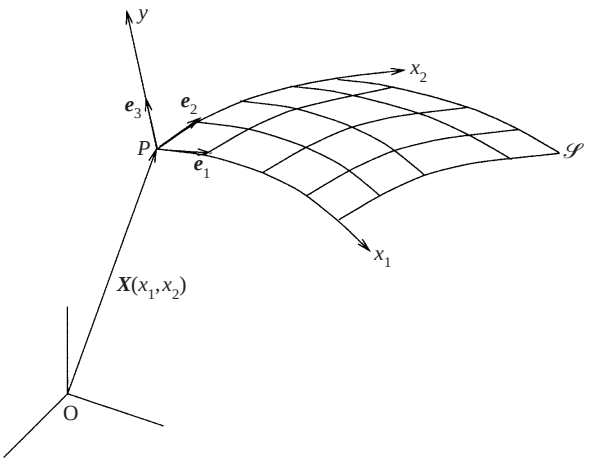

FIGURE 2. The substrate $\mathscr{S}$ is parameterized by variables x_1 and x_2. Together with the normal distance y, these form an orthogonal curvilinear coordinate system in space with unit vectors $\boldsymbol{e}_1$, $\boldsymbol{e}_2$ and $\boldsymbol{e}_3$.

We do not discuss boundary conditions at the lateral extremes of the substrate, as the substrate is assumed to be so large in extent, when compared to the fluid thickness, that the dynamics of the fluid film are largely unaffected by the edge boundary conditions. A rational methodology for deriving boundary conditions for slowly evolving dynamical models such as (1) is based upon constructing certain invariant manifolds of the dynamics as explained in Roberts (1992).

2.2. *The curvilinear coordinate system*

The curvilinear coordinate system is taken to be an extension into space of a natural coordinate system of the substrate. We choose, without loss of generality, a curvilinear parameterization (x_1, x_2) of $\mathscr{S}$ for which the parameter curves $x_1 =$ constant and $x_2 =$ constant generate the orthogonal lines of curvature of $\mathscr{S}$ (Stoker 1969), shown schematically in figure 2. In this case, the curvature tensor becomes diagonal everywhere, with diagonal components k_α.†

Conversely, we may view the surface $\mathscr{S}$ as being entirely specified by its metric coefficients $m_\alpha(x_1, x_2)$ and its principal curvatures $k_\alpha(x_1, x_2)$ as functions of the coordinate variables (x_1, x_2) assumed to generate the lines of curvature as the parameter curves of $\mathscr{S}$.

We also define the triad of unit orthogonal vectors $(\boldsymbol{e}_1, \boldsymbol{e}_2, \boldsymbol{e}_3)$ at all points of $\mathscr{S}$: $\boldsymbol{e}_\alpha$ is tangent to curves of constant $x_{\alpha'}$; and $\boldsymbol{e}_3$ is normal to $\mathscr{S}$. The metric coefficients, m_α, allow measurement of lengths on $\mathscr{S}$: the arclength of curves on the substrate are found from

$$\mathrm{d}s^2 = (m_1 \mathrm{d}x_1)^2 + (m_2 \mathrm{d}x_2)^2. \tag{9}$$

Note that the unit vectors vary along $\mathscr{S}$ and that their derivatives $\partial \boldsymbol{e}_i / \partial x_\alpha$ are required to express the equations of motion and boundary conditions in the curvilinear coordinates.

† Latin indices (such as i or j) span the numbers 1, 2, 3 and are attached to spatial quantities, whereas Greek indices (such as α or β) span the numbers 1, 2 and are attached to substrate or surface quantities. A prime on Greek indices denotes the complementary value, that is, $\alpha' = 3 - \alpha$. Subscripts following a comma indicate differentiation with respect to the corresponding coordinate. Unless otherwise specified, we do not use Einstein's summation convention for repeated indices.

As shown in figure 2, the two-dimensional substrate $\mathscr{S}$ is the locus of the endpoints of the position vector $\boldsymbol{r}_{OP} = \boldsymbol{X}(x_1, x_2)$, for some domain $\mathscr{D}$ of (x_1, x_2). We prescribe a third coordinate, denoted by y, as the distance measured along the normal $\boldsymbol{e}_3$ from a given spatial point P to the surface $\mathscr{S}$. Thus, the position vector of points P of the fluid are written

$$\boldsymbol{r} = \boldsymbol{X}(x_1, x_2) + y\boldsymbol{e}_3(x_1, x_2), \tag{10}$$

where the endpoint of vector $\boldsymbol{X}$ belongs to the surface $\mathscr{S}$. A large number of important simplifications occur in using this particular orthogonal curvilinear coordinate system, (x_1, x_2, y), that naturally fits the substrate. A definite example for the flow on a torus is given in § 5.4.

We denote by $\eta(t, x_1, x_2)$ the fluid layer's thickness at time t and location (x_1, x_2). The free surface $\mathscr{F}$ of the fluid is thus represented by the equation $y = \eta(t, x_1, x_2)$, and the fluid fills the domain $0 \leqslant y \leqslant \eta(t, x_1, x_2)$. Note that, in general, sufficiently far from the substrate for example, the chosen coordinate system need not lead to a one-to-one mapping between coordinate space and physical space. We assume that proper conditions between η, k_1 and k_2 are satisfied so that intersections of normals of $\mathscr{S}$ do not occur within the body of the fluid.

The coordinate unit vectors are independent of y and hence are the same unit vectors, $(\boldsymbol{e}_1, \boldsymbol{e}_2, \boldsymbol{e}_3)$, as defined on the substrate but now defined in space neighbouring $\mathscr{S}$. The corresponding spatial metric coefficients are

$$h_\alpha = m_\alpha(1 - k_\alpha y), \quad h_3 = 1. \tag{11}$$

By relating the base unit vectors of the rectangular coordinate system to those of the curvilinear coordinate system, see (Batchelor 1979 p. 598), or (Morse & Feshbach 1953), the spatial derivatives of the curvilinear unit vectors are

$$\boldsymbol{e}_{i,j} = \frac{\boldsymbol{e}_i}{h_i} h_{j,i} - \delta_{ij} \sum_{k=1}^{3} \frac{\boldsymbol{e}_k}{h_k} h_{i,k}. \tag{12}$$

However, in the special coordinate system used here, all such expressions simplify to the equivalent expressions on the substrate and independent of y:

$$\left.\begin{aligned} \boldsymbol{e}_{\alpha,\alpha} &= -\frac{m_{\alpha,\alpha'}}{m_{\alpha'}} \boldsymbol{e}_{\alpha'} + k_\alpha m_\alpha \boldsymbol{e}_3, & \boldsymbol{e}_{\alpha,\alpha'} &= \frac{m_{\alpha',\alpha}}{m_\alpha} \boldsymbol{e}_{\alpha'}, \\ \boldsymbol{e}_{3,\alpha} &= -k_\alpha m_\alpha \boldsymbol{e}_\alpha, & \boldsymbol{e}_{i,3} &= \boldsymbol{0}. \end{aligned}\right\} \tag{13}$$

This choice of curvilinear coordinates is required only for the derivation of an approximation of the dynamics of coating flow on $\mathscr{S}$. As seen in equation (1), for example, the model will be expressed ultimately in coordinate-free terms.

2.3. *Free-surface geometry*

The shape of the free surface is critical in thin-film flows; fluid surface curvature variations create pressure gradients to drive the fluid flow. To denote a quantity evaluated on the fluid's free surface we generally use a tilde (as in § 2.1).

The position of points P on the fluid's free surface $\mathscr{F}$ is given by

$$\boldsymbol{r}_{OP} = \tilde{\boldsymbol{X}}(x_1, x_2) = \boldsymbol{X}(x_1, x_2) + \eta(t, x_1, x_2)\boldsymbol{e}_3(x_1, x_2). \tag{14}$$

Hence, the surface $\mathscr{F}$ is naturally parameterized by (x_1, x_2). Its tangential vectors, $\tilde{\boldsymbol{t}}_1$ and $\tilde{\boldsymbol{t}}_2$, and unit normal vector, $\tilde{\boldsymbol{n}}$, are

$$\tilde{\boldsymbol{t}}_\alpha = \frac{\partial \tilde{\boldsymbol{X}}}{\partial x_\alpha} = \tilde{h}_\alpha \boldsymbol{e}_\alpha + \eta_{,\alpha} \boldsymbol{e}_3, \tag{15}$$

$$\tilde{\boldsymbol{n}} = \frac{\tilde{\boldsymbol{t}}_1 \times \tilde{\boldsymbol{t}}_2}{|\tilde{\boldsymbol{t}}_1 \times \tilde{\boldsymbol{t}}_2|} \propto -\tilde{h}_2\eta_{,1}\boldsymbol{e}_1 - \tilde{h}_1\eta_{,2}\boldsymbol{e}_2 + \tilde{h}_1\tilde{h}_2\boldsymbol{e}_3, \tag{16}$$

where $\tilde{h}_\alpha = m_\alpha(1 - k_\alpha\eta)$ are the metric coefficients at the free surface, and where $\eta_{,\alpha} = \partial\eta/\partial x_\alpha$.

At the free surface, $y = \eta$, the kinematic boundary condition must be imposed, namely, that fluid particles on the free surface remain on it. This leads to

$$\frac{\partial\eta}{\partial t} = v - \frac{u_1}{\tilde{h}_1}\frac{\partial\eta}{\partial x_1} - \frac{u_2}{\tilde{h}_2}\frac{\partial\eta}{\partial x_2} \quad \text{on} \quad \mathscr{F}. \tag{17}$$

To account for surface tension effects, we must compute the free surface mean curvature $\tilde{\kappa}$ in terms of the substrate principal curvatures and the film thickness η. A tractable route is to recognize that the effect of surface tension arises through the energy stored in the free surface. Thus, its contribution to the dynamical equations, through the surface curvature $\tilde{\kappa}$, arises from the variation of the surface area with respect to changes in the free-surface shape $y = \eta(t, x_1, x_2)$. The free-surface area is $A = \int \mathrm{d}A = \int \mathscr{A}\,\mathrm{d}x_1\mathrm{d}x_2$ where

$$\mathscr{A} = \sqrt{\tilde{h}_1^2\tilde{h}_2^2 + \tilde{h}_2^2\eta_{,1}^2 + \tilde{h}_1^2\eta_{,2}^2},$$

is proportional to the free-surface area above a patch $m_1\mathrm{d}x_1 \times m_2\mathrm{d}x_2$ of the substrate. The effect of curvature of the free surface, $\tilde{\kappa}$, is determined from the variation of $\mathscr{A}$ with respect to η:

$$\tilde{h}_1\tilde{h}_2\tilde{\kappa} = -\frac{\delta\mathscr{A}}{\delta\eta} = \frac{\partial}{\partial x_1}\left(\frac{\partial\mathscr{A}}{\partial\eta_{,1}}\right) + \frac{\partial}{\partial x_2}\left(\frac{\partial\mathscr{A}}{\partial\eta_{,2}}\right) - \frac{\partial\mathscr{A}}{\partial\eta}.$$

That is,

$$\begin{aligned}\tilde{\kappa} = {} & \frac{1}{\tilde{h}_1\tilde{h}_2}\left[\frac{\partial}{\partial x_1}\left(\frac{\tilde{h}_2^2\eta_{,1}}{\mathscr{A}}\right) + \frac{\partial}{\partial x_2}\left(\frac{\tilde{h}_2^2\eta_{,2}}{\mathscr{A}}\right)\right] \\ & + \frac{1}{\mathscr{A}}\left[(\tilde{h}_1^2 + \eta_{,1}^2)\frac{m_2k_2}{\tilde{h}_1} + (\tilde{h}_2^2 + \eta_{,2}^2)\frac{m_1k_1}{\tilde{h}_2}\right].\end{aligned} \tag{18}$$

An approximation is†

$$\tilde{\kappa} = \nabla^2\eta + \frac{k_1}{1 - k_1\eta} + \frac{k_2}{1 - k_2\eta} + O(\kappa^3 + \nabla^3\eta), \tag{19}$$

where it is sufficiently accurate to use the standard form of the Laplacian in the curvilinear coordinates of the substrate,

$$\nabla^2\eta = \frac{1}{m_1m_2}\left[\frac{\partial}{\partial x_1}\left(\frac{m_2}{m_1}\frac{\partial\eta}{\partial x_1}\right) + \frac{\partial}{\partial x_2}\left(\frac{m_1}{m_2}\frac{\partial\eta}{\partial x_2}\right)\right].$$

The approximation (19) arises directly from the form of the variational expression and accounts for changes in the free-surface curvature owing to the finite depth of the film, and variations in the film thickness.

† Some may argue that it is better to write $\tilde{\kappa} = \nabla^2\eta + \kappa + (k_1^2 + k_2^2)\eta + O(\kappa^3 + \nabla^3\eta)$. It is true that this form is just as consistent. However, the form (19) more accurately reflects the geometry of the curved substrate and at least on a cylinder, see § 5.3, seems crucial in modelling accurately the flow of thicker fluid films.

Note that throughout this paper, ∇ has two distinct meanings depending upon the context of whether it is applied to three-dimensional spatial fields, such as $\boldsymbol{u}$ and p, or to two-dimensional substrate fields such as η and κ.

3. Lubrication flow driven by surface tension

We now derive a model for the flow dynamics when the fluid film and the substrate vary on a large scale relative to the thickness of the film; because of the two vastly different space scales it may be viewed as a multiple-scale analysis. Viscous dissipation acts quickly across the fluid layer to damp out all except the slow dynamics associated with large-scale spreading. We assume that inertia and body forces are negligible, then by considering conservation of mass we derive an equation for the slow evolution of the film thickness η.

3.1. *Rescale the problem*

We rescale the non-dimensional governing equations. There are two characteristic lengths in the problem: a reference length L measured along the substrate and a reference thickness H of the fluid layer covering $\mathscr{S}$. The length scale L is thought of as either the scale of the radius of curvature of the substrate, or as the scale on which the film thickness varies. We generally expect both to be of a similar order of magnitude as they are both inversely proportional to substrate gradients, $\nabla \boldsymbol{n}$ and $\nabla\eta$, respectively. We denote the ratio H/L by ϵ, and assume $\epsilon \ll 1$ to be consistent with the thin-film/large-substrate assumption. In particular, we consider the flow to be non-dimensionally of thickness 1, and so the scale of lateral variations is non-dimensionally of large size $1/\epsilon$.

With the above in mind, we introduce the scaled curvatures (temporarily indicated by a superscript asterisk)

$$k_\alpha = \epsilon k_\alpha^*, \quad \tilde{\kappa} = \epsilon \tilde{\kappa}^*, \tag{20}$$

to express that the substrate and free-surface curvatures are $O(\epsilon)$. Then scale substrate coordinates and metric coefficients according to

$$m_\alpha = \tfrac{1}{\epsilon} m_\alpha^*, \quad x_\alpha^* = x_\alpha. \tag{21}$$

This form is appropriate if the substrate coordinates are naturally non-dimensional, such as the angular latitude and longitude coordinates on a sphere. (If you consider the substrate coordinates naturally as lengths, then the alternative scaling $m_\alpha = m_\alpha^*$, $x_\alpha^* = \epsilon x_\alpha$ is appropriate; whence one would consider x_α^* as a slow-space scale.) The rescaled spatial metric coefficients then become

$$h_\alpha^* = m_\alpha^*(1 - \epsilon k_\alpha^* y). \tag{22}$$

Seeking a slow flow leads to the following rescaling of the non-dimensional variables for pressure, velocity and stress:

$$p = \epsilon p^*, \quad u_\alpha = \epsilon^2 u_\alpha^*, \quad v = \epsilon^3 v^*, \quad \boldsymbol{\tau} = \epsilon^2 \boldsymbol{\tau}^*. \tag{23}$$

Now write the equations and boundary condition in the rescaled variables. In the following, for simplicity, we drop the superscript asterisk on all rescaled variables. First, the continuity equation, $\nabla \cdot \boldsymbol{u} = \boldsymbol{0}$,

$$\frac{\partial}{\partial x_1}(h_2 u_1) + \frac{\partial}{\partial x_2}(h_1 u_2) + \frac{\partial}{\partial y}(h_1 h_2 v) = 0, \tag{24}$$

then, the Stokes momentum equation, $\nabla p = \nabla^2 \boldsymbol{u}$:

$$\frac{\boldsymbol{e}_1}{h_1}\frac{\partial p}{\partial x_1} + \frac{\boldsymbol{e}_2}{h_2}\frac{\partial p}{\partial x_2} + \frac{1}{\epsilon}\boldsymbol{e}_3\frac{\partial p}{\partial y} = \frac{1}{h_1 h_2}\left\{\epsilon^2\frac{\partial}{\partial x_1}\left(\frac{h_2}{h_1}\frac{\partial}{\partial x_1}\right) + \epsilon^2\frac{\partial}{\partial x_2}\left(\frac{h_1}{h_2}\frac{\partial}{\partial x_2}\right) + \frac{\partial}{\partial y}\left(h_1 h_2\frac{\partial}{\partial y}\right)\right\}(u_1\boldsymbol{e}_1 + u_2\boldsymbol{e}_2 + \epsilon v\boldsymbol{e}_3). \quad (25)$$

The boundary conditions now take the following forms.

First, the no-slip boundary condition (6) is

$$u_i = 0 \quad \text{on} \quad y = 0. \quad (26)$$

Now consider the zero-shear-stress boundary condition at $y = \eta$. First, from (16), express the components of the normal unit vector $\tilde{\boldsymbol{n}}$ in terms of the scaled variables:

$$c\tilde{\boldsymbol{n}}_\alpha = -\epsilon(1 - \epsilon\eta k_{\alpha'})\frac{\eta_{,\alpha}}{m_\alpha}, \quad c\tilde{\boldsymbol{n}}_3 = (1 - \epsilon\eta k_1)(1 - \epsilon\eta k_2), \quad (27)$$

where $c = |\tilde{\boldsymbol{t}}_1 \times \tilde{\boldsymbol{t}}_2|$ is the constant of normalization. Furthermore, from Batchelor (1979 p. 599), the components of the non-dimensional (symmetric) deviatoric stress tensor, $\boldsymbol{\tau} = (\nabla\boldsymbol{u} + \nabla\boldsymbol{u}^{\mathrm{T}})$, become, upon scaling:

$$\left.\begin{aligned}
\tau_{\alpha\alpha} &= 2\epsilon\left[\frac{1}{m_\alpha}\frac{\partial u_\alpha}{\partial x_\alpha} + \frac{m_{\alpha,\alpha'}}{m_1 m_2}u_{\alpha'}\right] + O(\epsilon^2),\\
\tau_{12} &= \epsilon\left[\frac{1}{m_2}\frac{\partial u_1}{\partial x_2} + \frac{1}{m_1}\frac{\partial u_2}{\partial x_1} - \frac{m_{1,2}}{m_1 m_2}u_1 - \frac{m_{2,1}}{m_1 m_2}u_2\right] + O(\epsilon^2),\\
\tau_{\alpha 3} &= \frac{\partial u_\alpha}{\partial y} + \epsilon k_\alpha u_\alpha + O(\epsilon^2),\\
\tau_{33} &= 2\epsilon\frac{\partial v}{\partial y}.
\end{aligned}\right\} \quad (28)$$

Thus, correct to order ϵ, the only contributing terms in the boundary condition $\tilde{\boldsymbol{\tau}} \cdot \tilde{\boldsymbol{t}}_\alpha = 0$ is $\tau_{\alpha 3}\tilde{\eta}_3$, namely

$$\frac{\partial u_\alpha}{\partial y} + \epsilon k_\alpha u_\alpha + O(\epsilon^2) = 0. \quad (29)$$

In order to write down the normal stress boundary condition on the free surface, equation (8), we must first express the free surface mean curvature $\tilde{\kappa}$ correct to order ϵ: from (19), we write here the scaled free-surface mean curvature as

$$\tilde{\kappa} = \kappa + \epsilon\kappa_2\eta + \epsilon\nabla^2\eta + O(\epsilon^2),$$

where $\kappa = k_1 + k_2$ and $\kappa_2 = k_1^2 + k_2^2$. Next, the normal surface stress component to order ϵ^2 in scaled form is (using summation)

$$-p + \epsilon\tilde{n}_i\tilde{n}_j\tau_{ij} = -p + 2\epsilon^2\left(\frac{\partial v}{\partial y} - \frac{\eta_{,1}}{m_1}\frac{\partial u_1}{\partial y} - \frac{\eta_{,2}}{m_2}\frac{\partial u_2}{\partial y}\right) + O(\epsilon^3).$$

Hence, the normal stress condition (8) becomes

$$p = -\kappa - \epsilon\kappa_2\eta - \epsilon\nabla^2\eta + O(\epsilon^2) \quad \text{on} \quad y = \eta; \quad (30)$$

viscous stresses have no influence on the normal stress to this order in this scaling.

3.2. *Perturbation solution*

We now find a solution of these equations by assuming a perturbation expansion of the unknown fields in terms of the small parameter ϵ. We write each component in

the following expansion:

$$\left.\begin{aligned} u_\alpha &= u_\alpha^{(0)} + \epsilon u_\alpha^{(1)} + \epsilon^2 u_\alpha^{(2)} + \cdots, \\ v &= v^{(0)} + \epsilon v^{(1)} + \epsilon^2 v^{(2)} + \cdots, \\ p &= p^{(0)} + \epsilon p^{(1)} + \epsilon^2 p^{(2)} + \cdots. \end{aligned}\right\} \tag{31}$$

Then, at the leading order, we find the following equations governing $u_\alpha^{(0)}$, $v^{(0)}$ and $p^{(0)}$:

$$\left.\begin{aligned} &\frac{\partial p^{(0)}}{\partial y} = 0, \quad \frac{\partial^2 u_\alpha^{(0)}}{\partial y^2} = \frac{1}{m_\alpha}\frac{\partial p^{(0)}}{\partial x_\alpha}, \\ &\frac{\partial}{\partial x_1}(m_2 u_1^{(0)}) + \frac{\partial}{\partial x_2}(m_1 u_2^{(0)}) + m_1 m_2 \frac{\partial v^{(0)}}{\partial y} = 0, \end{aligned}\right\} \tag{32}$$

with the boundary conditions

$$\left.\begin{aligned} &u_\alpha^{(0)} = v^{(0)} = 0 \quad \text{at} \quad y = 0, \\ &\frac{\partial u_\alpha^{(0)}}{\partial y} = 0, \quad p^{(0)} = -\kappa \quad \text{at} \quad y = \eta. \end{aligned}\right\} \tag{33}$$

The solution of these equations is readily found to be the expected locally parabolic flow driven by pressure gradients induced by substrate curvature variations:

$$\left.\begin{aligned} p^{(0)} &= -\kappa, \\ u_\alpha^{(0)} &= -\frac{1}{m_\alpha}\kappa_{,\alpha}(\tfrac{1}{2}y^2 - \eta y), \\ v^{(0)} &= \nabla^2\kappa(\tfrac{1}{6}y^3 - \tfrac{1}{2}\eta y^2) - \tfrac{1}{2}\nabla\kappa\cdot\nabla\eta\, y^2. \end{aligned}\right\} \tag{34}$$

If the substrate has constant mean curvature, such as a cylinder (§ 5.3) or a sphere, then there is no flow at this order – flow occurs at the next order.

At the next order of perturbation:

$$\left.\begin{aligned} &\frac{\partial p^{(1)}}{\partial y} = 0, \quad \frac{\partial^2 u_\alpha^{(1)}}{\partial y^2} - \kappa\frac{\partial u_\alpha^{(0)}}{\partial y} = \frac{1}{m_\alpha}\left(\frac{\partial p^{(1)}}{\partial x_\alpha} + k_\alpha y\frac{\partial p^{(0)}}{\partial x_\alpha}\right), \\ &\frac{\partial}{\partial x_1}(m_2 u_1^{(1)}) + \frac{\partial}{\partial x_2}(m_1 u_2^{(1)}) + m_1 m_2\frac{\partial v^{(1)}}{\partial y} = 0, \end{aligned}\right\} \tag{35}$$

with boundary conditions

$$\left.\begin{aligned} &u_\alpha^{(1)} = v^{(1)} = 0 \quad \text{at} \quad y = 0, \\ &\frac{\partial u_\alpha^{(1)}}{\partial y} = -k_\alpha u_\alpha^{(0)}, \quad p^{(1)} = -(\kappa_2\eta + \nabla^2\eta) \quad \text{at} \quad y = \eta. \end{aligned}\right\} \tag{36}$$

We solve these equations to find

$$\left.\begin{aligned} p^{(1)} &= -(\kappa_2\eta + \nabla^2\eta), \\ u_\alpha^{(1)} &= -\frac{1}{m_\alpha}(\kappa_2\eta + \nabla^2\eta)_{,\alpha}(\tfrac{1}{2}y^2 - \eta y) - \frac{k_\alpha}{6m_\alpha}\kappa_{,\alpha}y^3 \\ &\quad -\frac{\kappa}{m_\alpha}\kappa_{,\alpha}(\tfrac{1}{6}y^3 - \tfrac{1}{2}\eta y^2 + \tfrac{1}{2}\eta^2 y), \end{aligned}\right\} \tag{37}$$

and $v^{(1)}$ which is not recorded here as it is not subsequently needed.

3.3. *Conservation of mass*

The expressions in the previous subsection show how the velocity and pressure fields respond to free-surface and substrate curvature. Such flow will thin the film in some places and thicken it in others (see § 5). Conservation of fluid then leads us to an expression for the evolution of the film's thickness η by the driven flow. Initially, we work with non-dimensional but unscaled variables and coordinates before returning to scaled quantities.

Consider a small volume above a patch of the substrate extending across the fluid layer from $y = 0$ to $y = \eta$, see figure 3. It is bounded by the substrate, the instantaneous free surface and the coordinate surfaces x_1, $x_1 + \mathrm{d}x_1$, x_2, $x_2 + \mathrm{d}x_2$. The rate at which fluid leaves this volume is expressed to first order of infinitesimal quantities $\mathrm{d}x_1$ and $\mathrm{d}x_2$ as the sum of three terms: first,

$$\int_0^{\eta(x_1+\mathrm{d}x_1,x_2)} [u_1 h_2 \mathrm{d}x_2]_{x_1+\mathrm{d}x_1} \mathrm{d}y - \int_0^{\eta(x_1,x_2)} [u_1 h_2 \mathrm{d}x_2]_{x_1} \mathrm{d}y, \tag{38}$$

for the surfaces x_1 and $x_1 + \mathrm{d}x_1$; secondly, a corresponding term for the surfaces x_2 and $x_2 + \mathrm{d}x_2$; and lastly, the term

$$\int_{\mathscr{F}} \boldsymbol{u} \cdot \tilde{\boldsymbol{n}} \, \mathrm{d}S = \{\tilde{h}_1 \tilde{h}_2 v - \eta_{,1} \tilde{h}_2 u_1 - \eta_{,2} \tilde{h}_1 u_2\} \mathrm{d}x_1 \mathrm{d}x_2 = \tilde{h}_1 \tilde{h}_2 \frac{\partial \eta}{\partial t} \mathrm{d}x_1 \mathrm{d}x_2, \tag{39}$$

for the bounding free surface $\mathscr{F}$, where we have used the kinematic boundary condition (17). Upon dividing by $\mathrm{d}x_1 \mathrm{d}x_2$ and in the limit of $\mathrm{d}x_1 \mathrm{d}x_2 \to 0$, we deduce

$$m_1 m_2 (1 - \eta k_1)(1 - \eta k_2) \frac{\partial \eta}{\partial t} = -\frac{\partial}{\partial x_1}(m_2 Q_1) - \frac{\partial}{\partial x_2}(m_1 Q_2), \tag{40}$$

where the Q_α terms are the components of the total flux of fluid over a position on the substrate, defined as

$$\boldsymbol{Q}(t, x_1, x_2) = Q_1 \boldsymbol{e}_1 + Q_2 \boldsymbol{e}_2 = \int_0^{\eta} ((1 - k_2 y) u_1 \boldsymbol{e}_1 + (1 - k_1 y) u_2 \boldsymbol{e}_2) \mathrm{d}y. \tag{41}$$

After division of (40) by $m_1 m_2$, recognize on the right-hand side the surface divergence of the flux vector $\boldsymbol{Q}$ expressed in the orthogonal curvilinear coordinate system of $\mathscr{S}$. This yields the divergence form of the conservation of mass equation:

$$(1 - \eta k_1)(1 - \eta k_2) \frac{\partial \eta}{\partial t} = -\frac{1}{m_1 m_2} \left(\frac{\partial}{\partial x_1}(m_2 Q_1) + \frac{\partial}{\partial x_2}(m_1 Q_2) \right) = -\nabla \cdot \boldsymbol{Q}. \tag{42}$$

We find an approximation of the flux vector $\boldsymbol{Q}$ by taking into account the thin-layer characteristics of the flow over $\mathscr{S}$, as determined earlier.

Returning to the rescaled quantities introduced in § 3.1, we now determine the perturbation coefficients of the flux vector $\boldsymbol{Q} = \epsilon^2 \boldsymbol{Q}^{(0)} + \epsilon^3 \boldsymbol{Q}^{(1)} + \cdots$ to be

$$\boldsymbol{Q}^{(0)} = \int_0^{\eta} (u_1^{(0)} \boldsymbol{e}_1 + u_2^{(0)} \boldsymbol{e}_2) \mathrm{d}y = \tfrac{1}{3} \eta^3 \left(\frac{\boldsymbol{e}_1}{m_1} \kappa_{,1} + \frac{\boldsymbol{e}_2}{m_2} \kappa_{,2} \right) = \tfrac{1}{3} \eta^3 \nabla \kappa, \tag{43}$$

$$\begin{aligned} \boldsymbol{Q}^{(1)} &= \int_0^{\eta} ((u_1^{(1)} - k_2 y u_1^{(0)}) \boldsymbol{e}_1 + (u_2^{(1)} - k_1 y u_2^{(0)}) \boldsymbol{e}_2) \mathrm{d}y \\ &= \tfrac{1}{3} \eta^3 \nabla (\kappa_2 \eta + \nabla^2 \eta) + \tfrac{1}{6} \eta^4 \boldsymbol{K} \cdot \nabla \kappa - \tfrac{1}{3} \eta^4 \kappa \nabla \kappa, \end{aligned} \tag{44}$$

where $\boldsymbol{K} = k_\alpha \delta_{\alpha\beta} (\boldsymbol{e}_\alpha : \boldsymbol{e}_\beta)$ is the curvature tensor (which would not be diagonal in a general orthogonal coordinate system of the substrate $\mathscr{S}$).

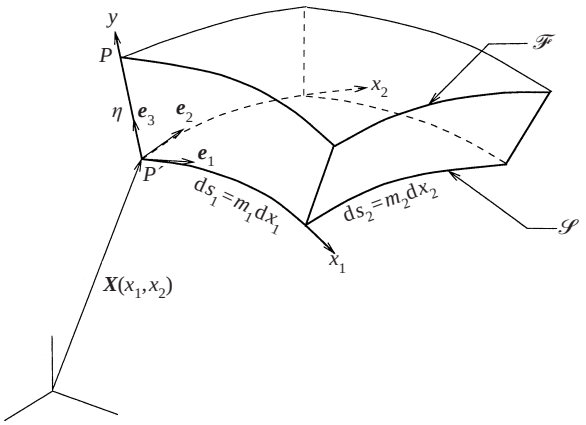

FIGURE 3. A small control volume V bounded by the substrate, $\mathscr{S}$, the free surface, $\mathscr{F}$, and four coordinate surfaces with separation $m_1 \mathrm{d}x_1$ and $m_2 \mathrm{d}x_2$.

Finally, the corresponding evolution equation for the film thickness η, the so-called lubrication approximation, is

$$(1-\epsilon\eta k_1)(1-\epsilon\eta k_2)\frac{\partial \eta}{\partial t} = -\tfrac{1}{3}\epsilon^3 \nabla\cdot[\eta^3\nabla\tilde{\kappa} - \epsilon\eta^4\kappa\nabla\kappa + \tfrac{1}{2}\epsilon\eta^4 \boldsymbol{K}\cdot\nabla\kappa] + O(\epsilon^5), \qquad (45)$$

where $\tilde{\kappa} = \kappa + \epsilon\kappa_2\eta + \epsilon\nabla^2\eta + O(\epsilon^2)$ or given by (19). We express this equation in the more convenient form

$$\frac{\partial \zeta}{\partial t} = -\tfrac{1}{3}\epsilon^3 \nabla\cdot[\eta^2\zeta\nabla\tilde{\kappa} - \tfrac{1}{2}\epsilon\eta^4(\kappa \boldsymbol{I} - \boldsymbol{K})\cdot\nabla\kappa] + O(\epsilon^5), \qquad (46)$$

where $\zeta = \eta - \frac{1}{2}\epsilon\kappa\eta^2 + \frac{1}{3}\epsilon^2 k_1 k_2 \eta^3$ is proportional to the amount of fluid in the film lying 'above' a patch of the substrate. Rewriting this in terms of unscaled, non-dimensional quantities gives (1) when the free-surface curvature is approximated by an expression such as (19).

4. Systematic modelling involving gravity and inertia

The previous analysis based upon traditional scaling arguments gives a limited model for the dynamics of the film thickness. However, it is not straightforward to extend such an analysis for generally curved substrates in the presence of variously competing physical effects such as gravity and inertia. In this section, we appeal to the more powerful centre manifold theory to extend the previous model in order to include a gravitational body force and to determine the leading influence of inertia. Gravity is also an important effect included. Oron *et al.* (1997 p. 975) identify that modelling of inertia is crucial in at least two circumstances: in film rupture and in falling films (Chang 1994). Inertia is also significant in regions of the flow on a spinning disk (Oron *et al.* 1997 p. 954). The centre manifold approach we employ here provides strong theoretical support for the development of low-dimensional models of fluid dynamics (Procaccia 1988, for example). The systematic nature of the approach also lends itself well towards the computer algebra we employed. The analysis is based upon viscously decaying shear flow being forced by large-scale physical effects. Centre

manifold theory guarantees fidelity between model and original equations. This leads to the correct modelling (Suslov & Roberts 1998) of initial conditions (3) and forcing; no other method does this but we do not develop these aspects here. This section also serves as an example of the analysis that may be undertaken if other physical processes affect the lubrication dynamics.

4.1. *Basis of the centre manifold*

Centre manifold theory (Carr 1981) assures us that the long-term dynamics near a fixed point of a dynamical system may be accurately described by a 'low-dimensional' model. Here, the lubrication model (1) is, of low-dimension in comparison to that of the incompressible Navier–Stokes equations, (4) and (5). The first task is to establish the linear basis, here due to the viscous decay of shear flow, for the application of centre manifold theory to support the lubrication model.

Analogous to the approach developed by Roberts (1996, 1998), we retain the small parameter ϵ introduced in § 3.1 and scale the curvatures and metric coefficients according to (20) and (21). By considering ϵ negligible, we, in the preliminary linear analysis, restrict attention to large-scale flows on a flat substrate. However, we do not explicitly scale the dependent fields, p and $\boldsymbol{u}$ as in (23), because in this approach their scaling naturally arises from the dynamical equations during the course of the analysis rather than being imposed at the outset – this is an essential feature for deriving a model valid over a wide range of competing physical effects. Formally, we treat lateral derivatives and gravity as small effects by substituting, as in Roberts (1998), the Bond number $Bo = \beta^2$, then adjoining the trivial equations

$$\frac{\partial \epsilon}{\partial t} = \frac{\partial \beta}{\partial t} = 0, \tag{47}$$

to the scaled versions of the fluid equations (4) and (5) and their boundary conditions. Here, the Reynolds number is unrestricted, it is not assumed small. Then all terms involving products of $\boldsymbol{u}$, ϵ and β are perturbing nonlinear terms (as in the analysis of the unfolding of bifurcations (Carr 1981) or in analyses using the slowly varying approximation (Roberts 1988)).

Such nonlinear terms are discarded in the preliminary linear analysis to leave linear equations

$$\nabla \cdot \boldsymbol{u} = 0, \quad Re\frac{\partial \boldsymbol{u}}{\partial t} + \nabla p - \nabla^2 \boldsymbol{u} = \boldsymbol{0}, \tag{48}$$

where, since $\epsilon = 0$, in effect, these differential operators are the Cartesian operators appropriate to a flat substrate. These equations are to be solved with boundary conditions of $\boldsymbol{u} = \boldsymbol{0}$ on $\mathscr{S}(y = 0)$ and

$$\frac{\partial \eta}{\partial t} - v = 0, \quad \frac{\partial u_\alpha}{\partial y} = p - 2\frac{\partial v}{\partial y} = 0 \quad \text{on} \quad y = \eta. \tag{49}$$

All solutions of these linear equations are composed of the decaying lateral shear modes, $v = p = 0$, $u_\alpha = c_\alpha \sin(l\pi y/(2\eta))\exp(\lambda t)$ for odd integers l, together and independently with $\eta =$ constant, $u_\alpha = v = p = 0$. In these modes, the decay-rate in time is $\lambda = -l^2\pi^2/(4\eta^2 Re)$, except for the last mentioned mode which, as a consequence of fluid conservation, has a decay rate $\lambda = 0$. So linearly, and in the absence of any lateral variations on a flat substrate, all the lateral shear modes decay exponentially quickly, the slowest on a non-dimensional time scale of $4Re\eta^2/\pi^2$, just leaving a film of constant thickness as the long-lasting mode. This spectrum, of

all eigenvalues being strictly negative except for a few that are zero, is the classic spectrum for the application of centre manifold theory. The existence theorem 1 in Carr (1981) assures us that the nonlinear effects just perturb the linear picture of the dynamics so that there exists a low-dimensional model parameterized by the film thickness η. The relevance theorem 2 in Carr (1981) assures us that this model is exponentially quickly attractive to all nearby fluid flows and so forms a generic model of the long-term fluid dynamics of the film; for example, this theorem supports that the initial condition (3) ensures long-term agreement between the lubrication model and the fluid flow. With the caveat that strict theory has not yet been extended sufficiently to cover this particular application, the closest being that of Gallay (1993) and Hărăguş (1996) (but also see Roberts 1988), recognise that this theory provides the strongest support for the lubrication model of fluid flow that is currently available.

We apply the centre manifold concepts and techniques to systematically develop the low-dimensional lubrication model of the dynamics of the film. Having identified the critical mode associated with the zero decay rate, the subsequent analysis is straightforward. The approach is to write the fluid fields $\boldsymbol{v}(t) = (u_1, u_2, v, p)$ as a function of the critical mode η (effectively equivalent to the 'slaving' principle of synergetics, Haken 1983). Instead of seeking asymptotic expansions in the 'amplitude' of the critical mode (see, for example, Roberts 1988; Mercer & Roberts 1990; Roberts 1996), we apply an iterative algorithm to find the centre manifold and the evolution there on which is based directly upon the approximation theorem 3 in Carr (1981) and Roberts (1997) and its variants, as explained in detail by Roberts (1997). We seek solutions for the fluid fields as

$$\boldsymbol{v}(t) = \boldsymbol{V}(\eta), \quad \text{such that} \quad \frac{\partial \eta}{\partial t} = G(\eta, \boldsymbol{V}(\eta)), \tag{50}$$

where dependence upon the constant parameters (ϵ, β) is implicit, and where G is the right-hand side of the rescaled version of the kinematic condition (17). The iterative scheme (see Roberts 1997) finds the physical fields $\boldsymbol{v}(t)$ that form actual solutions of the scaled Navier–Stokes equations; this ensures fidelity between the model and the fluid dynamics. The iteration is repeated, in computer algebra,† until the residual of the Navier–Stokes equations and boundary conditions becomes zero to some order of error, whence the model will be accurate to the same order of error (by the centre manifold approximation theorem 3 in Carr 1981). Thus, the key to the correctness of the results produced by the computer algebra is the proper coding of the fluid dynamical equations in the curvilinear coordinate system. Upon obtaining the code,‡ these can be seen in the computed residuals within the iterative loop.

4.2. *The general lubrication model*

Based upon the scalings introduced in § 3.1, we run the REDUCE computer algebra program that computes velocity and pressure fields for the flow and the evolution equation for the film's thickness. We find that the evolution equation may be written

† The computer algebra package REDUCE was used because of its flexible 'operator' facility. At the time of writing, information about REDUCE was available from Anthony C. Hearn, RAND, Santa Monica, CA 90407-2138, USA; e-mail: reduce@rand.org.

‡ The source code is publicly available via http://www.sci.usq.edu.au/staff/robertsa or by contacting A.J.R.

in the coordinate-free form†

$$\begin{aligned}\frac{\partial\zeta}{\partial t} = &-\tfrac{1}{3}\epsilon^3\nabla\cdot[\eta^2\zeta\nabla\tilde{\kappa} - \tfrac{1}{2}\epsilon\eta^4(\kappa\boldsymbol{I}-\boldsymbol{K})\cdot\nabla\kappa]\\ &-\tfrac{1}{3}\epsilon Bo\nabla\cdot[\eta^3\hat{\boldsymbol{g}}_s - \epsilon\eta^4(\kappa\boldsymbol{I}+\tfrac{1}{2}\boldsymbol{K})\cdot\hat{\boldsymbol{g}}_s + \epsilon\hat{g}_y\eta^3\nabla\eta]\\ &+O(\epsilon^5+Bo^{5/2}),\end{aligned} \tag{51}$$

where $\hat{\boldsymbol{g}}_s$ and $\hat{g}_y$ are, respectively, the components of the gravitational unit vector tangent and normal to the substrate. Recall that $\zeta = \eta - \frac{1}{2}\kappa\eta^2 + \frac{1}{3}k_1k_2\eta^3$ and that the mean curvature of the fluid surface $\tilde{\kappa}$ is approximated by (19). Note that in the special orthogonal curvilinear system used in the derivation of the model,

$$\kappa\boldsymbol{I}-\boldsymbol{K} = \begin{bmatrix} k_2 & 0\\ 0 & k_1\end{bmatrix}, \quad \kappa\boldsymbol{I}+\tfrac{1}{2}\boldsymbol{K} = \begin{bmatrix} \frac{3}{2}k_1+k_2 & 0\\ 0 & k_1+\frac{3}{2}k_2\end{bmatrix}.$$

Flows on examples of curved substrates are discussed in the next section.

The general model, (51), is derived solely under the assumptions that curvature and free-surface slopes, as measured by ϵ, and the gravitational forcing, measured by the Bond number Bo, are perturbing influences. The application of centre manifold theory places no restrictions upon their relative magnitudes – we do not have to insist on $Bo \sim \epsilon$ or any other such relation between these two independent parameters. Provided there are no 'run away' instabilities, the model is valid over any scaling regime where both parameters are small. In particular, the model is valid as the tangential and normal gravitational forcing vary widely around a curving substrate, and is valid whether the mean substrate curvature, often the leading-order effect, is zero or not.

Also note that the model (51) was derived without placing any overt restriction upon the Reynolds number, it was treated as an $O(1)$ constant. That the model actually turns out to have no Reynolds number dependence just confirms the Stokes flow nature of these lubrication dynamics. Higher-order analysis, as also seen in Roberts (1998 §4), shows that the Reynolds number first appears at $O(\epsilon^6+Bo^3)$ for fluid films. Thus, inertia is formally negligible. However, if the Reynolds number is large enough to be significant, then we have determined that the following $O(Re\epsilon^6+ReBo^3)$ terms could be included in the evolution equation, (51):

$$\begin{aligned}\frac{\partial\zeta}{\partial t} = &\cdots\\ &-\frac{Re\epsilon^6}{5}\nabla\cdot\left[\frac{2\eta^6}{3}(\nabla\eta\cdot\nabla\kappa)\nabla\kappa - \frac{\eta^7}{7}\nabla(\nabla\kappa\cdot\nabla\kappa) + \frac{26\eta^7}{63}(\nabla^2\kappa)\nabla\kappa\right]\\ &-\frac{2Re\epsilon^4Bo}{15}\nabla\cdot\left[\eta^6(\hat{\boldsymbol{g}}_s\cdot\nabla\eta\nabla\kappa + \hat{\boldsymbol{g}}_s\nabla\eta\cdot\nabla\kappa) - \frac{3\eta^7}{7}\nabla(\hat{\boldsymbol{g}}_s\cdot\nabla\kappa)\right.\\ &\qquad\left.+\frac{13\eta^7}{21}\hat{\boldsymbol{g}}_s\nabla^2\kappa + \frac{13\eta^7}{21}\hat{g}_y\kappa\nabla\kappa\right]\\ &-\frac{2Re\,\epsilon^2Bo^2}{15}\nabla\cdot\left[\eta^6\hat{\boldsymbol{g}}_s(\hat{\boldsymbol{g}}_s\cdot\nabla\eta) + \frac{\eta^7}{21}(13\kappa\boldsymbol{I}-9\boldsymbol{K})\cdot\hat{\boldsymbol{g}}_s\hat{g}_y\right].\end{aligned} \tag{52}$$

See that for a flat substrate ($k_1 = k_2 = 0$), these Reynolds number correction terms

† $O(\epsilon^p+Bo^q)$ is used to denote terms, z, for which $z/(\epsilon^p+Bo^q)$ is bounded as $(\epsilon, Bo)\to 0$. The upshot is that $z=\epsilon^mBo^n$ is $O(\epsilon^p+Bo^q)$ only if $m/p+n/q \geqslant 1$. For example, an expression accurate to $O(\epsilon^5+Bo^{5/2})$ retains all terms of the form ϵ^mBo^n for $m+2n<5$.

reduce to those derived by Benney (1966) and Atherton & Homsy (1976). We suggest, as do Oron *et al.* (1997 p. 975), that these higher-order terms are most likely to be used to estimate the error in the lubrication model, (51), when applied to moderate Reynolds number flows. Thus, these expressions may be used to indicate when a more sophisticated dynamical model, such as a two-mode model (Chang 1994; Roberts 1996; Li & Roberts 1999), is required in order to resolve the inertial instabilities of fluid films at higher Reynolds numbers.

Of course, an order of magnitude argument will give a global estimate, over space and time, of the influence of inertia. However, we may make a perfectly satisfactory *a priori* order of magnitude assessment, but if in a simulation an instability grows, then the terms in (52) will detect if it grows too large. Thus, (52) supplements order of magnitude estimates by giving focused local estimates of inertia-induced errors in any actual simulation.

5. Example film flows on curved substrates

In this section, we use the preceding lubrication models to demonstrate some of the flow effects caused by substrate curvature.

5.1. *Qualitative effect of substrate curvature*

Equation (46) shows that, to leading order of perturbation, the flow is driven by substrate curvature gradients, curvature caused by film thickness variations is generally smaller unless the substrate is comparatively gently curved. To appreciate the effect of substrate curvature qualitatively, consider a two-dimensional flow on a one-dimensional substrate with given curvature $\kappa(x_1)$. Denote $x = x_1$ as substrate arclength so that the scale factor $m_1 = 1$ and there are no variations in x_2. Then, to leading order and in the absence of body forces, the flow is governed by the first-order partial differential equation for η:

$$(1 - \kappa\eta)\frac{\partial \eta}{\partial t} = -\frac{1}{3}\frac{\partial}{\partial x}(\eta^3 \kappa_x). \tag{53}$$

This has a characteristic solution

$$\dot{x} = \kappa_x \frac{\eta^2}{1 - \kappa\eta}, \quad \dot{\eta} = -\tfrac{1}{3}\kappa_{xx}\frac{\eta^3}{1 - \kappa\eta}. \tag{54}$$

Wherever the substrate curvature κ has a local minimum, say at $x = x_0$, then

$$\kappa_x < 0\,(x < x_0), \quad \kappa_x > 0\,(x > x_0), \quad \kappa_{xx} > 0.$$

Thus, according to the characteristic equations, the flow is thinned in the neighbourhood of $x = x_0$. Indeed, since $\eta \propto -\kappa_{xx}\eta^3$, the film thickness η typically decreases as $t^{-1/2}$ at a point of minimum curvature ($\kappa_{xx} > 0$). As shown schematically in figure 4, this thinning applies in the neighbourhood of minimum absolute curvature for exterior coating flows, and of maximum absolute curvature for exterior coating flows.

Conversely, the film thickens in the neighbourhood of a point of maximum mean curvature, as also shown in figure 4. The characteristic solution (54) predicts a film thickness that blows up in finite time. The role of higher-order terms in the model equation (1) is to smooth out such singularities induced by structurally unstable, low-order models such as (53).

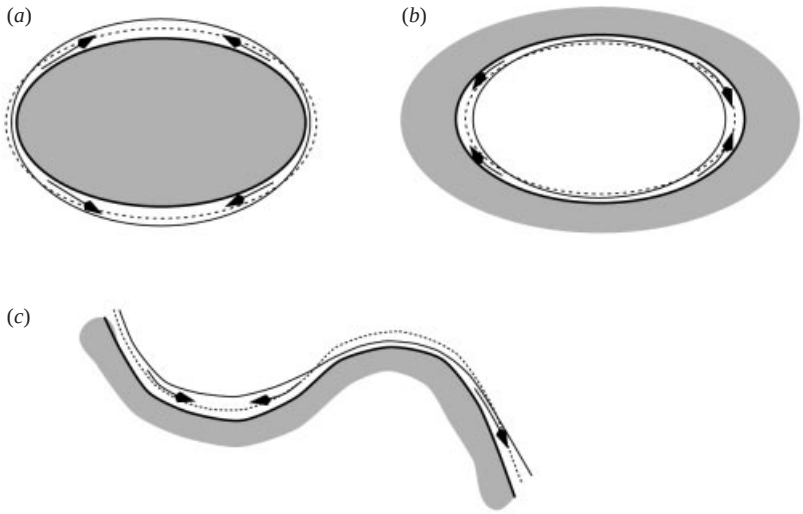

FIGURE 4. Leading effects of substrate curvature on the evolution of a thin flow.

5.2. *Corner flow*

Consider here the two-dimensional fluid flow examined by Schwartz & Weidner (1995) consisting of the flow which thins a film around an outside corner, as shown in figure 5. The fluid is taken to have surface tension $\sigma = 30\,\mathrm{dyn\,cm^{-1}}$, viscosity $\mu = 1$ poise, and density $\rho = 1\,\mathrm{g\,cm^{-3}}$. Initially, the film is a uniform 0.01 cm thick, corresponding to a Reynolds number of $Re = 0.003$, around the corner which has a radius of 0.1 cm. (Dimensional units are used to facilitate comparison with Schwartz & Weidner 1995.) As in the previous subsection, the most convenient way to parameterize the one-dimensional substrate is in terms of the arclength x. In this case, our dynamical model (1) reduces to

$$\frac{\partial\zeta}{\partial t} = (1-\kappa\eta)\frac{\partial\eta}{\partial t} = -\frac{1}{3}\frac{\partial}{\partial x}\left[\eta^2\zeta\frac{\partial\tilde{\kappa}}{\partial x}\right], \tag{55}$$

where $\tilde{\kappa} \approx \kappa + \kappa^2\eta + (\partial^2\eta/\partial x^2)$, and $\kappa = k_1(x)$ is the curvature of the substrate. In contrast, the model of Schwartz & Weidner (the SaW model) is

$$\frac{\partial\eta}{\partial t} = -\frac{1}{3}\frac{\partial}{\partial x}\left[\eta^3\frac{\partial}{\partial x}\left(\kappa + \frac{\partial^2\eta}{\partial x^2}\right)\right]. \tag{56}$$

The differences between the models are that ours includes more terms in the curvature. In particular, ours conserves fluid whereas the SaW model does not. Indeed, in the course of the numerical simulations of the film flow shown in figure 5, the SaW model lost about 2% of the fluid, whereas ours lost none to within computational error. For thicker films the difference is more marked.

A numerical scheme to simulate a fluid film via these equations is straightforward. We approximated both (55) and (56) by finite differences on a spatial grid with $N = 97$ points and, because the dynamics are stiff, we employed an implicit integration scheme with time step $\Delta t = 0.00115\,\mathrm{s}$. The numerical scheme uses second-order centred differences in space and time, but, in the interests of speed, the nonlinear coefficients are only computed from the earlier time. By varying the size of the space–time grid we determined that these parameters give a numerically accurate simulation.

Shown in figures 6 and 7 are comparisons between the predictions of the SaW model

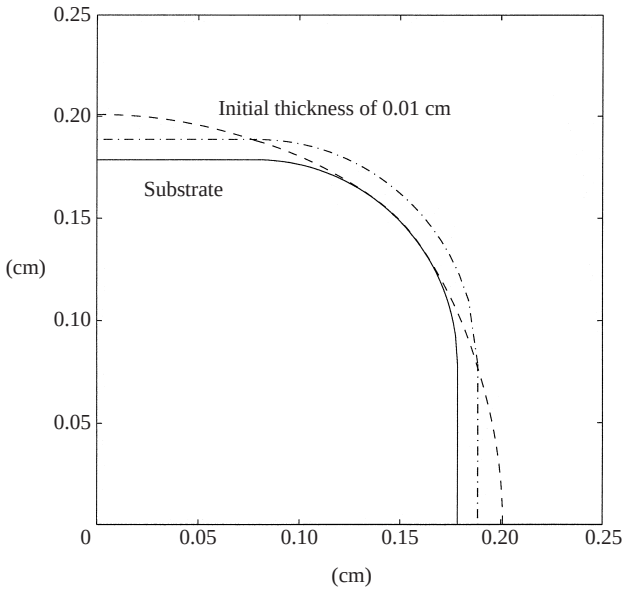

FIGURE 5. Coating flow on an outside corner at 300 s. The initial film of fluid (dot-dashed) of constant thickness around a corner (solid) evolves over a long time to thin around the corner (dashed). (Unlike Schwartz & Weidner (1995) figure 7, the thickness of the film has not been exaggerated.)

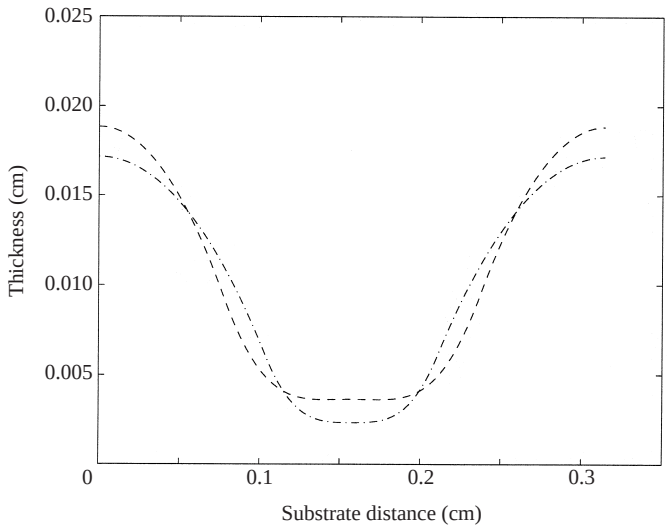

FIGURE 6. Film thickness for the flow around the corner shown in figure 5 at time $t = 3$ s: — — —, our model (55); —·—, SaW model (56).

and ours during the simulation of the thinning of the film around the corner. Observe that the SaW model and ours are quantitatively different: the SaW model predicts a more rapid thinning of the film around the corner, and a slower thickening of the film away from the corner. For example, the thickness at $x = 0$ and $t = 3$ s for our model is only reached by the SaW model at time $t \approx 300$ s. For quantitative accuracy the thin-film flows require the extra curvature terms employed in our model (55).

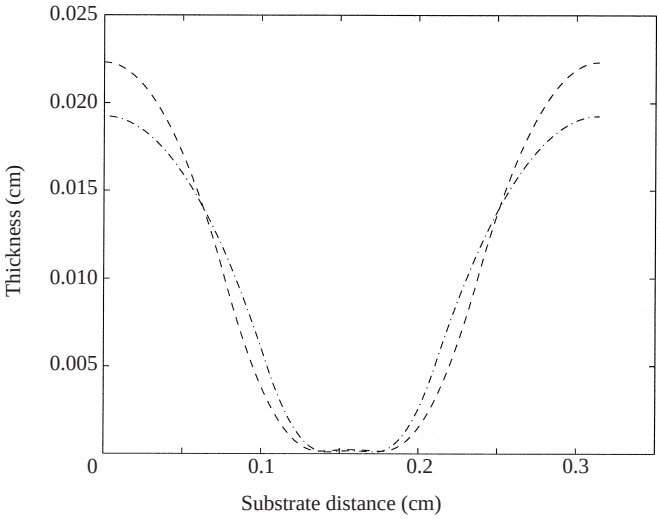

FIGURE 7. Film thickness for the flow around the corner shown in fiugre 5 at time $t = 300\,\mathrm{s}$: – – –, our model (55); —·—, SaW model (56).

5.3. *Flow on a circular cylinder*

One example of the application of the general model (51) is to the dynamics of thin films on vertical cylinders or fibres as introduced briefly in § 1. The flow on a cylinder is perhaps the most common example of a curved substrate (for example, Frenkel 1992; Kalliadasis & Chang 1994; Jensen 1997; Oron *et al.* 1997; Weidner, Schwartz & Eres 1997; Kliakhandler *et al.* 2001). Here, we elaborate on the discussion in § 1 and provide more substantive details.

The version of the general model, (51), specific to axisymmetric flow down a cylinder of radius a is the model (2). Now consider the flow on a cylinder of radius a at arbitrary orientation. Let the axial coordinate be $x = x_1$ and the angular coordinate $\theta = x_2$ then the curvatures $k_1 = 0$ and $k_2 = -1/a$ and the substrate scale factors $m_1 = 1$ and $m_2 = a$ – flow on the outside of a cylinder is described with positive a, and that on the inside of the cylinder with negative a. The local direction cosines of the gravity vector in the axial, angular and radial directions are denoted by $\hat{g}_x$, $\hat{g}_\theta$ and $\hat{g}_y$, respectively – the latter two vary with angle θ. In terms of the fluid fluxes and $\zeta = \eta + \eta^2/2a$, the general model (51) is

$$\frac{\partial \zeta}{\partial t} = -\nabla \cdot \boldsymbol{Q} = -\frac{\partial Q_x}{\partial x} - \frac{1}{a}\frac{\partial Q_\theta}{\partial \theta}, \tag{57}$$

where

$$Q_x = \tfrac{1}{3}\eta^2\zeta\left[\frac{1}{a^2(1+\eta/a)^2}\eta_x + \eta_{xxx} + \frac{1}{a^2}\eta_{x\theta\theta}\right] + \frac{Bo}{3}\eta^3[\hat{g}_x(1+\eta/a) + \hat{g}_y\eta_x]$$

and

$$Q_\theta = \tfrac{1}{3}\eta^2\zeta\left[\frac{1}{a^3(1+\eta/a)^2}\eta_\theta + \frac{1}{a}\eta_{xx\theta} + \frac{1}{a^3}\eta_{\theta\theta\theta}\right] + \frac{Bo}{3}\eta^3\left[\hat{g}_\theta(1+3\eta/2a) + \hat{g}_y\frac{1}{a}\eta_\theta\right].$$

Having constant mean curvature, there is no flow of the sort discussed in § 5.1 driven directly by the substrate curvature. As noted by others, the principal effect of the substrate curvature on a cylinder, the first term in the above fluxes, is akin to that of a radial gravitational field away from the substrate, as seen in the last term in the above

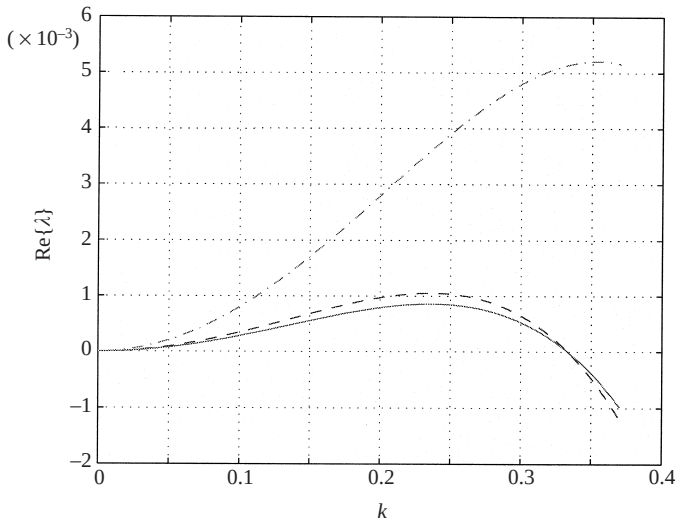

FIGURE 8. Real part of the growth rate of disturbances to an axisymmetric, fluid film of thickness 1 draining down a cylinder of radium $a = 2$: for —·—, the Frenkel model (2) in Kalliadasis & Chang (1994); · · ·, RRS model (2); and — — —, KDB model (5.5) in Kliakhandler *et al.* (2001). Our model (2) agrees best with the exact numerical solutions in Kliakhandler *et al.* (2001) figure 3(*b*).

fluxes. For very thin fluid films, $\eta/a \ll 1$, the above model matches with earlier axisymmetric models on vertical cylinders (e.g. Frenkel 1992; Kalliadasis & Chang 1994), and axially invariant models on horizontal cylinders (e.g. Oron *et al.* 1997 equation (2.108)). The differences lie in the extra terms to account for the physical interactions that take place in thicker films and the generalization to non-symmetric flows.

The model in equation (57) restricted to axisymmetric flows was reported in §1 as (2). Differences were identified between our model and earlier models for films on cylinders of relatively small radius; an example was shown in figure 1. Kliakhandler *et al.* (2001) recently heuristically derived a lubrication model for axisymmetric films on thin cylinders (the KDB model, Kliakhandler *et al.* 2001 equation (5.3)) and compared their model predictions to those obtained numerically for the linear dynamics of perturbations to a constant thickness film. Both their model and ours predict, for disturbances $\eta - 1 \propto \mathrm{e}^{\mathrm{i}kx+\lambda t}$, a growth rate in the form

$$\lambda = A\left[\frac{k^2}{(1+a)^2} - k^4\right]; \tag{58}$$

but their coefficient A (Kliakhandler *et al.* equation (5.6)) is much more complicated than ours:

$$A = \frac{a + \frac{1}{2}}{3(a+1)}. \tag{59}$$

The growth rates, (58), are plotted in figure 8 along with that for the earlier Frenkel model (Kalliadasis & Chang 1994 equation (2)). On a cylinder of radius twice the fluid thickness, the KDB model and ours are very similar, with ours appearing to be a better match to the exact numerics plotted in figure 3(*b*) of Kliakhandler *et al.* (2001); whereas the Frenkel model is much worse, being in error by a factor of 6 in growth rate and 2 in wavenumber. Crucial in the agreement between our model, the KDB model and the numerical simulations is the presence of the $(1+a)^2$ denominator in (58) which is absent in other models such as Frenkel's: the factor

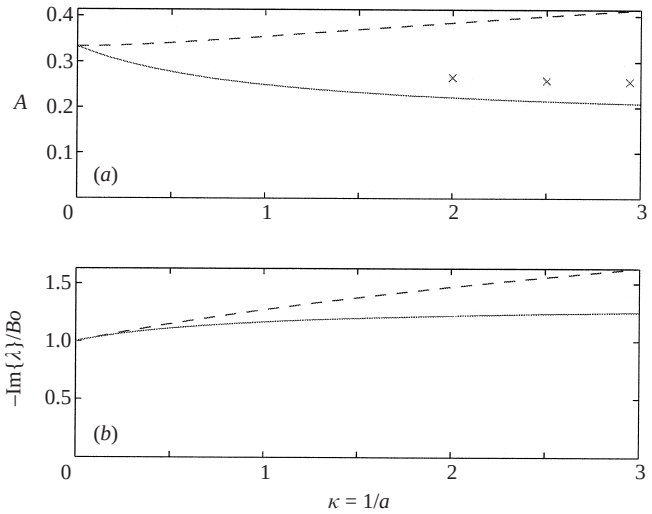

FIGURE 9. (*a*) Comparison of the coefficient A (Kliakhandler *et al.* 2001 equation (5.6)) for – – –, the KDB model, and ——, our RRS model (59), showing that our coefficient leads to a much improved match with exact numerics represented by the three crosses from digitizing the maxima of figure 3(*a*) in Kliakhandler *et al.* (2001). (*b*) Shows that the phase speed of the linear roll waves is similar in the two models.

arises precisely because we approximate the free surface mean curvature by (19) with the denominators $1-k_1\eta$ and $1-k_2\eta$ intact to account more fully for the effects of substrate curvature. Thus, the longer roll waves seen in our simulations of figure 1(*b*) are almost certain to be reasonably accurate.

The small differences in linear stability of our model and the KDB model seen above for radius $a=2$ are more marked when compared to the actual experiments of Kliakhandler *et al.* (2001) where the mean fluid film was two to three times as thick as the cylinder radius. In figure 9, we plot the coefficient A of the growth rate (58) for our model (59) and for the KDB model (their equation (5.6)) as a function of the cylindrical substrate curvature $\kappa=1/a$; the differences grow with curvature κ (figure 8 corresponds to $\kappa=0.5$). Also plotted in figure 9 is a measure of the amplitude of three exact factors obtained from the relative heights of the maximum of the three numerical curves given in figure 3(*a*) of Kliakhandler *et al.* (2001): see that the growth rates for our model more closely match the exact values than does the KDB model. Our model (57) for the flow on a cylindrical substrate appears to perform the best of any in its class.

5.4. *Flow around a torus*

Here we discuss the evolution of the flow over the surface of a torus with tube of radius R_2 and centreline of radius R_1. We use the following parameterization:

$$\left.\begin{aligned} X_1 &= (R_1+R_2\cos\theta)\cos\phi,\\ X_2 &= (R_1+R_2\cos\theta)\sin\phi,\\ X_3 &= R_2\sin\theta. \end{aligned}\right\} \tag{60}$$

Take $R_2<R_1$ to avoid self-intersection, and denote the coordinates $x_1=\phi$ and $x_2=\theta$ with $0\leqslant\phi<2\pi$ and $0\leqslant\theta<2\pi$. Then, this parameterization generates an orthogonal curvilinear coordinate system with corresponding orthonormal basis

vectors:

$$\left.\begin{aligned} \boldsymbol{e}_1 &= \boldsymbol{e}_\phi = -\sin\phi\,\boldsymbol{i} + \cos\phi\,\boldsymbol{j}, \\ \boldsymbol{e}_2 &= \boldsymbol{e}_\theta = -\sin\theta(\cos\phi\,\boldsymbol{i} + \sin\phi\,\boldsymbol{j}) + \cos\theta\,\boldsymbol{k}, \\ \boldsymbol{e}_3 &= \boldsymbol{e}_1 \times \boldsymbol{e}_2 = \cos\theta(\cos\phi\,\boldsymbol{i} + \sin\phi\,\boldsymbol{j}) + \sin\theta\,\boldsymbol{k}, \end{aligned}\right\} \tag{61}$$

in terms of the unit vectors of the conventional Cartesian coordinate system, and with the corresponding surface metrics

$$m_1 = m_\phi = R_1 + R_2\cos\theta, \quad m_2 = m_\theta = R_2. \tag{62}$$

The chosen coordinate system also generates lines of principal curvature as the parameter curves. We then obtain the following principal curvatures and mean curvature:

$$k_1 = -\frac{\cos\theta}{R_1 + R_2\cos\theta}, \quad k_2 = -\frac{1}{R_2}, \quad \kappa = -\frac{1}{R_2}\frac{R_1 + 2R_2\cos\theta}{R_1 + R_2\cos\theta}. \tag{63}$$

The mean curvature of the substrate is maximum at the inner rim of the torus ($\theta = \pi$), and minimum at the outer rim ($\theta = 0$). Hence, we expect the fluid layer to thicken around the inner rim, and to thin around the outer, solely due to surface tension effects.

We solve the model (46) numerically. For simplicity, we seek axisymmetric solutions, that is, solutions independent of the angle ϕ around the rim of the torus, and so the film thickness depends only upon θ, the angle around the tube, and time t. We try the following form for

$$\eta(t,\theta) = \sum_{n=0}^{N-1} a_n(t)\cos(n\theta), \tag{64}$$

which guarantees the periodicity of the solution and imposes symmetry across the plane $z = 0$. The ordinary differential equations for the coefficients a_n are found by a Galerkin method where they are determined by making the corresponding residual error orthogonal to the N basis functions, $\cos(n\theta)$, in the usual L_2 norm. As a check, we confirm that the total volume enclosed between the free surface of the fluid and the toroidal substrate remains constant in time. Two numerical simulations were carried out.

First, we start with an initially uniform layer of thickness $\eta_0 = 0.1$ on a torus with $R_1 = 2$ and $R_2 = 1$. The corresponding flow towards the inner rim of the torus is shown by the evolution of the film thickness in figure 10.

Secondly, we simulated the flow evolving from a strip of fluid placed around the outer rim of the torus. Again, as shown in figure 11, the fluid flows around to the inner rim.

On the torus, the effects of inertia on this lubrication flow are estimated by the ratio between typical values of the right-hand side of (46) and that of (52); dominantly,

$$\text{inertia} : \text{lubrication} \approx \frac{Re\,\eta^4}{6R_1R_2^2}.$$

As may be expected, a thicker film or a more sharply curved torus are more likely to be affected by such higher-order influences. Note that for flows inside a toroidal tube, the thinning of the liquid layer occurs around the inner rim ($\theta = \pi$).

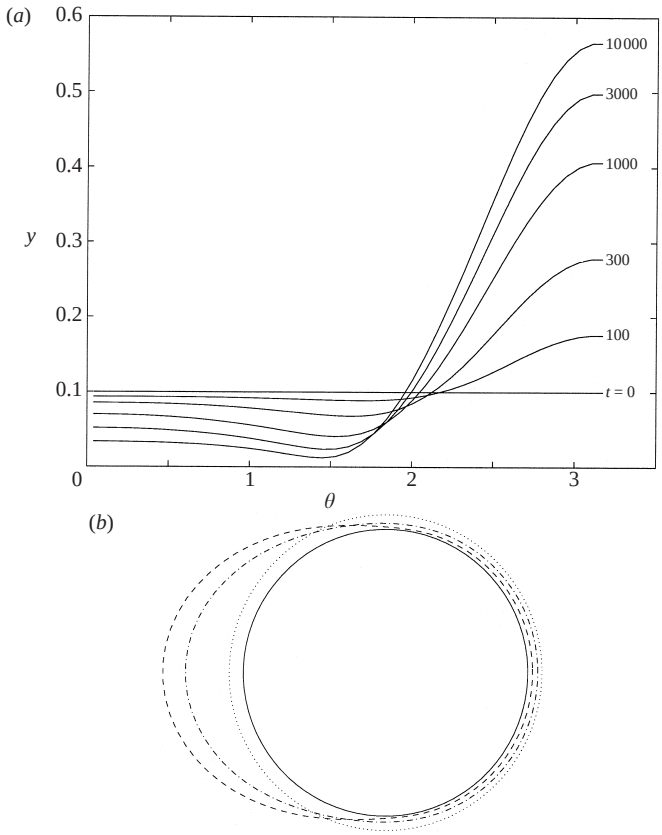

FIGURE 10. Evolution of flow on the surface of a torus with $N = 15$ terms in Galerkin approximation. $R_1 = 2$, $R_2 = 1$, $\eta_0 = 0.1$: (*a*) $\eta(t, \theta)$ shown at $t = 0$, 100, 300, 1000, 3000, 10 000; (*b*) initial, intermediate ($t = 1000$) and late ($t = 10\,000$) stages of the film on a cross-section of the torus.

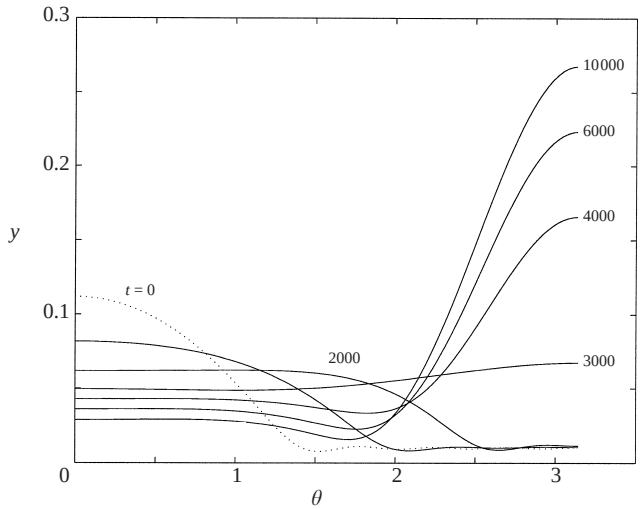

FIGURE 11. Same as figure 10 with a step-like initial layer (dotted). $N = 15$ and $t = 0$, 1000, 2000, 3000, 4000, 6000, 8000, 10 000.

6. Conclusion

The model, (1), applies to a wide range of thin fluid film flows in the lubrication approximation on curved substrates, and its generalization, (51), includes gravitational effects. The models are derived by faithfully satisfying the Navier–Stokes equations for a Newtonian fluid expressed in a coordinate system fitted to the curved substrate (§ 2). The first derivation is based upon fluid conservation (§ 3), whereas the second more general derivation is based upon the centre manifold approach (§ 4). We have commented on the issues resolved by using the centre manifold approach rather than traditional approaches such as multiple scales or indeed simple heuristics: the assurance of exponential quick applicability of the model (e.g. Carr 1981) and its order of error; the novel and proper projection of initial conditions, (3), from (Suslov & Roberts 1998), the possible provision of correct boundary conditions (Roberts 1992); and the more sophisticated modelling of thin fluid films involving the dynamics of momentum (Roberts 1996, 1998). Such a theoretically sound approach is essential for further developments of fluid modelling.

Models for the flow on some specific substrates (§ 5) are obtained directly from (1) or (51), with both constant and varying mean substrate curvature. For example, the model, (57), for flow on a circular cylinder appears to perform better than any earlier model (e.g. Frenkel 1992; Kliakhandler *et al.* 2001). All models have errors. In particular, we have derived a quantitative estimate of the error, (52), incurred in neglecting inertia in thin fluid film flow. Such quantitative estimates will better determine when more sophisticated models of the fluid flow are necessary.

R. V. R. acknowledges his many helpful discussions with L. W. Schwartz. His work was done while spending a sabbatical leave at USQ whose warm hospitality is also gratefully acknowledged. A. J. R. acknowledges the support of a grant from the Australian Research Council.

REFERENCES

Atherton, R. W. & Homsy, G. M. 1976 On the derivation of evolution equations for interfacial waves. *Chem. Engng Commun.* **2**, 57–77.

Batchelor, G. K. 1979 *An Introduction to Fluid Dynamics.* Cambridge University Press.

Benney D. J. 1966 Long waves on liquid films. *J. Maths & Phys.* **45**, 150–155.

Cairncross, R. A., Francis, L. F. & Scriven, L. E. 1996 Predicting drying in coatings that react and gel-drying regime maps. *AIChE J.* **42**, 55–67.

Carr, J. 1981 *Applications of Centre Manifold Theory, Appl. Math. Sci.* vol. 35. Springer.

Chang, H. C. 1994 Wave evolution on a falling film. *Annu. Rev. Fluid Mech.* **26**, 103–136.

Cox, S. M. & Roberts, A. J. 1991 Centre manifolds of forced dynamical systems. *J. Austral. Math. Soc.* B **32**, 401–436.

Cox, S. M. & Roberts, A. J. 1995 Initial conditions for models of dynamical systems. *Physica* D **85**, 126–141.

van de Fliert, B. W., Howell, P. D. & Ockenden, J. R. 1995 Pressure-driven flow of a thin viscous sheet. *J. Fluid Mech.* **292**, 359–376.

Frenkel, A. L. 1992 Nonlinear theory of strongly undulating thin films flowing down vertical cylinders. *Europhys. Lett.* **18**, 583–588.

Frenkel, A. L. & Indireshkumar, K. 1997 Wavy film flows down an inclined plane. Part 1. Perturbation theory and general evolution equation. Tech. Rep. University of Alabama. http://arXiv.org/abs/patt-sol/9712005.

Gallay, Th. 1993 A center-stable manifold theorem for differential equations in Banach spaces. *Commun. Math. Phys.* **152**, 249–268.

Grotberg, J. B. 1994 Pulmonary flow and transport phenomena. *Annu. Rev. Fluid Mech.* **26**, 529–571.

Haken, H. 1983 *Synergetics, an Introduction.* Springer.

Hăr ăguş, M. 1996 Model equations for water waves in the presence of surface tension. *Eur. J. Mech.* **15**, 471–492.

Jensen, O. E. 1997 The thin liquid lining of a weakly curved cylindrical tube. *J. Fluid Mech.* **331**, 373–403.

Kalliadasis, S. & Chang, H.-C. 1994 Drop formation during coating of vertical fibres. *J. Fluid Mech.* **261**, 135–168.

Kliakhandler, I. L., Davis, S. H. & Bankoff, S. G. 2001 Viscous beads on vertical fibre. *J. Fluid Mech.* **429**, 381–390.

Levich, V. G. 1962 *Physicochemical Hydrodynamics.* Prentice-Hall.

Li, Z. & Roberts, A. J. 1999 The accurate and comprehensive model of thin fluid flows with inertia on curved substrates. Tech. Rep. June, http://arXiv.org/abs/chao-dyn/9906011.

Mei, C. C. 1989 *The Applied Dynamics of Ocean Surface Waves, Advanced Series on Ocean Engineering,* vol. 1. World Scientific.

Mercer, G. N. & Roberts, A. J. 1990 A centre manifold description of contaminant dispersion in channels with varying flow properties. *SIAM J. Appl. Maths* **50**, 1547–1565.

Moriarty, J. A. & Schwartz, L. W. 1992 Effective slip in numerical calculations of moving-contact line problems. *J. Engng Maths* **26**, 81–86.

Moriarty, J. A. & Schwartz, L. W. 1993 Dynamic considerations in the closing and opening of holes in thin liquid films. *J. Colloid Interface Sci.* **161**, 335–342.

Moriarty, J. A., Schwartz, L. W. & Tuck, E. O. 1991 Unsteady spreading of thin liquid films with small surface tension. *Phys. Fluids* A **3**, 733–742.

Morse, P. & Feshbach, H. 1953 *Methods of Mathematical Physics.* McGraw-Hill.

Oron, A., Davis, S. H. & Bankoff, S. G. 1997 Long-scale evolution of thin liquid films. *Rev. Mod. Phys.* **69**, 931–980.

Procaccia, I. 1988 Weather systems: complex or just complicated? *Nature* **333**, 498–499.

Ribe, N. M. 2001 Bending and stretching of thin viscous sheets. *J. Fluid Mech.* **433**, 135–160.

Roberts, A. J. 1988 The application of centre manifold theory to the evolution of systems which vary slowly in space. *J. Austral. Math. Soc.* B **29**, 480–500.

Roberts, A. J. 1992 Boundary conditions for approximate differential equations. *J. Austral. Math. Soc.* B **34**, 54–80.

Roberts, A. J. 1993 The invariant manifold of beam deformations. Part 1. The simple circular rod. *J. Elas.* **30**, 1–54.

Roberts, A. J. 1996 Low-dimensional models of thin film fluid dynamics. *Phys. Letts.* A **212**, 63–72.

Roberts, A. J. 1997 Low-dimensional modelling of dynamical systems. Tech. Rep. http://arXiv.org/abs/chao-dyn/9705010.

Roberts, A. J. 1997 Low-dimensional modelling of dynamics via computer algebra. *Comput. Phys. Commun.* **100**, 215–230.

Roberts, A. J. 1998 An accurate model of thin 2d fluid flows with inertia on curved surfaces. In *Free Surface Flows with Viscosity* (ed. P. A. Tyvand). Advances in Fluid Mechanics, vol. 16 chap. 3, pp. 69–88. Comput. Mech. Pub.

Roberts, A. J. 2000 Computer algebra derives correct initial conditions for low-dimensional dynamical models. *Comput. Phys. Commun.* **126**, 187–206.

Roberts, A. J. 2001 Holistic projection of initial conditions onto a finite difference approximation. *Comput. Phys. Commun.* (to appear) http://arXiv.org/abs/math.NA/0101205.

Roskes, G. J. 1969 Three-dimensional long waves on a liquid film. *Phys. Fluids* **13**, 1440–1445.

Ruschak, K. J. 1985 Coating flows. *Annu. Rev. Fluid Mech.* **17**, 65–89.

Schwartz, L. W., Cairncross, R. A. & Weidner, D. E. 1996 Anomalous behavior during leveling of thin coating layers with surfactants. *Phys. Fluids* A **8**, 1693–1695.

Schwartz, L. W. & Weidner, D. E. 1995 Modeling of coating flows on curved surfaces. *J. Engng Maths* **29**, 91–103.

Schwartz, L. W., Weidner, D. E. & Eley, R. R. 1995 An analysis of the effect of surfactant on the levelling behaviour of a thin coating layer. *Langmuir* **11**, 3690–3693.

Stoker, J. J. 1969 *Differential Geometry.* Wiley-Interscience.

Suslov, S. A. & Roberts, A. J. 1998 Proper initial conditions for the lubrication model of thin film fluid flow. Preprint 1998.

Sweeney, J. B., Davis, T., Scriven, L. E. & Zasadzinski, J. A. 1993 Equilibrium thin films on rough surfaces. 1. Capillary and disjoining effects. *Langmuir* **9**, 1551–1555.

Timoshenko, S. P. & Woinowsky-Krieger, S. 1959 *Theory of Shells and Plates.* McGraw-Hill.

Tuck, E. O. & Schwartz, L. W. 1990 A numerical and asymptotic study of some third-order ODEs relevant to draining and coating flows. *SIAM Rev.* **32**, 453–469.

Watt, S. D. & Roberts, A. J. 1995 The accurate dynamic modelling of contaminant dispersion in channels. *SIAM J. Appl. Maths* **55**, 1016–1038.

Weidner, D. E. & Schwartz, L. W. 1994 Contact-line motion of shear-thinning liquids. *Phys. Fluids* **6**, 3535–3538.

Weidner, D. E., Schwartz, L. W. & Eley, R. R. 1996 Role of surface tension gradients in correcting coating defects in corners. *J. Colloid Interface Sci.* **179**, 66–75.

Weidner, D. E., Schwartz, L. W. & Eres, M. H. 1997 Simulation of coating layer evolution and drop formation on horizontal cylinders. *J. Colloid Interface Sci.* **187**, 243–258.

Wilson, S. K. & Duffy, B. R. 1998 On the gravity-driven draining of a rivulet of viscous fluid down a slowly varying substrate with variation transverse to the direction of flow. *Phys. Fluids* **10**, 13–22.